IEEE Access
Multidisciplinary | Rapid Review | Open Access Journal

Received September 24, 2019, accepted October 9, 2019, date of publication October 17, 2019, date of current version October 30, 2019.

Digital Object Identifier 10.1109/ACCESS.2019.2948091

JSSA: Joint Sidelobe Suppression Approach for Collaborative Beamforming in Wireless Sensor Networks

SHUANG LIANG[1], ZHIYI FANG[1], GENG SUN[1, 2, 3], (Member, IEEE), YANHENG LIU[1], XIAOHUI ZHAO[3], (Member, IEEE), GUANNAN QU[1], (Member, IEEE), YING ZHANG[4], (Senior Member, IEEE), AND VICTOR C. M. LEUNG[5, 6], (Fellow, IEEE)

[1]College of Computer Science and Technology, Jilin University, Changchun 130012, China
[2]Key Laboratory of Symbolic Computation and Knowledge Engineering of Ministry of Education, Jilin University, Changchun 130012, China
[3]College of Communication Engineering, Jilin University, Changchun 130012, China
[4]School of Electrical and Computer Engineering, Georgia Institute of Technology, Atlanta, GA 30332, USA
[5]Department of Electrical and Computer Engineering, The University of British Columbia, Vancouver, BC V6T 1Z4, Canada
[6]College of Computer Science and Software Engineering, Shenzhen University, Shenzhen 518061, China

Corresponding author: Geng Sun (sungeng@jlu.edu.cn)

This work was supported in part by the National Natural Science Foundation of China under Grant 61872158, in part by the National Science Foundation for Young Scientists of China under Grant 61806083, in part by the Postdoctoral Innovative Talent Support Program of China, in part by the China Postdoctoral Science Foundation under Grant 2018M640283, and in part by the Science and Technology Development Plan Project of Jilin Province under Grant 20190701019GH.

ABSTRACT Conventional collaborative beamforming (CB) with virtual node antenna array often results in high maximum sidelobe level (SLL) due to the unexpected positions of the nodes. In this paper, a sidelobe suppression approach (JSSA) to suppress the maximum SLL by jointly optimizing the locations and amplitude weights of the nodes is proposed. JSSA organizes the node positions according to the concentric circular antenna array for location optimization. Then, a novel algorithm called variation particle chicken swarm optimization (VPCSO) is proposed to further optimize the amplitude weights of the selected CB nodes. The proposed VPCSO introduces the variation mechanism and location learning mechanism to enhance the performance of the conventional chicken swarm optimization algorithm. Simulations are conducted and the results show that the proposed location optimization approach is effective, and the maximum SLLs of beam patterns obtained by VPCSO are lower than that of other algorithms. Moreover, the energy consumption can be saved by VPCSO. In addition, electromagnetic (EM) simulations are conducted to verify the performance of the proposed JSSA in EM environments.

INDEX TERMS Collaborative beamforming, beam pattern, sidelobe level, swarm intelligence optimization, wireless sensor networks.

I. INTRODUCTION

With the rapid development of the Internet of Things (IoT) and the increasing number of the intelligent devices, wireless sensor networks (WSNs) are widely used for objective monitoring as an important component of IoT [1]–[5]. WSNs are characterized by a huge number of sensor nodes that randomly deployed in a wide sensing field [6], [7]. In practical applications, the amplitude of the nodes is limited because of the limitations in size and energy of the nodes [8]. Thus, the multi-hop has to be used to enhance the communication distance between a sensor node and a base station (BS) [9]. However, this results in the increased communication delay and the reduced reliability [10]. In addition, replenishing the energy to the sensors is always difficult because of the limited application environment [11]. Therefore, to improve the communication distance and to reduce the energy consumption have become important issues in WSNs.

To improve the communication distance of a single node, the sensor nodes are able to form a virtual node antenna array (VNAA) and then communicate with the BS directly through collaborative beamforming (CB) [12]–[14]. The nodes in a VNAA can be divided into the source node and the array nodes [14], respectively, and they could transmit the

The associate editor coordinating the review of this manuscript and approving it for publication was Shah Nawaz Burokur.

common data for up-link communications. Moreover, if N nodes communicate with the BS through CB, then N^2 gains can be obtained at the target location according to the superposition principle of electromagnetic wave [13]–[15]. The shapes of the conventional antenna array are fixed, however, the sensor nodes are usually distributed in the monitoring area randomly. Thus, compare to the fixed shape antenna arrays, the VNAA composed of randomly located nodes cause higher sidelobe level (SLL) of the beam patterns [16], [17], which also increases the interference and reduces the amplitude concentration of the mainlobe. Therefore, to suppress the maximum SLL of the VNAA caused by the random distributed nodes has become the pivotal problem in effectively utilizing CB.

In the antenna arrays, several parameters can be controlled for the beam pattern synthesis such as the phase and the amplitude of the elements [18]–[20]. The authors in [21] propose a maximum SLL reduction method to suppress the SLL of the VNAA. This method utilizes a node selection approach by testing various combinations of the CB nodes. Chen et al. [16] propose an CB array node optimization mechanism based on the cross-entropy optimization for the maximum SLL reductions of CB. In reference [22], the nulls are obtained in a certain direction of the beam patterns through adjusting the phase of each antenna element. The authors in [23] present a particle swarm optimization (PSO)-based algorithm to calculate the distances between the array nodes to achieve a lower maximum SLL. In the above mentioned work, the amplitude weight of each node in the CB array are all uniform.

However, the nodes cannot be moved after they are deployed in many applications. Thus, the conventional method for optimizing the array node spacings does not work well. Moreover, the amplitude of the CB array nodes is another a key factor that directly affects the beam patterns. Recently, the nature-inspired approaches such as the evolutionary computation and swarm intelligence optimization algorithms become one of the main approaches for the antenna array amplitude optimizations. For example, the PSO algorithm [24], the genetic algorithm (GA) [25], the firefly algorithm (FA) [26], the cuckoo search (CS) algorithm [27] and the biogeography-based optimization (BBO) [28] have been applied for the beam pattern optimizations of the fixed shape antenna arrays. However, a sensor node in IoT usually has limited computing capacity. Thus, an optimization approach has to have a higher accuracy and a faster convergence rate for the beam pattern optimizations of CB, thereby reducing the computing time and the communication delay.

The main contributions of this work are summarized as follows:

- We propose a joint sidelobe suppression approach (JSSA) for optimizing the locations and amplitude weights of the array nodes in CB.
- We propose a concentric circular antenna array (CCAA)-based array node selection mechanism in JSSA for the location optimizations. Then, a novel nature-inspired algorithm, namely, variation particle chicken swarm optimization (VPCSO), is proposed to determine the better amplitude weights of the selected array nodes after the location optimization. VPCSO introduces the position learning mechanism and the variation mechanism into the conventional chicken swarm optimization (CSO), where the former can improve the convergence rate and the latter is able to improve the accuracy.
- Several extended simulations are conducted for the verification of proposed JSSA. Moreover, we also conduct electromagnetic (EM) simulations to evaluate the performance of JSSA in approximate practical applications.

A. ROADMAP

The rest of the paper is organized as follows. Section II introduces the system models. Section III proposes JSSA. Section IV gives the simulation results and Section V concludes the paper.

II. SYSTEM MODELS

A. NETWORK MODEL

We assume that a WSN is covered by several isomorphic smart devices (sensor nodes). The work ID of each node is unique and the location coordinates of each node is known, this can be achieved by several methods, e.g., a GPS module. Moreover, all the nodes are statics which means that they cannot move after initial deployment.

In addition, the network also has the following characteristics [6], [15], [16], [21]:

A1: Each sensor node has a single omnidirectional antenna.

A2: The maximum amplitude of all the nodes are the same, and hence the nodes have the same communication radius (R_c). Moreover, the amplitude weight of each node is adjustable.

A3: Only uplink transmission by using CB is considered since the downlink communications that from the BS to sensor nodes do not have big challenge.

A4: The network as well as the sensor nodes are synchronized including the time, the carrier frequency and the initial phase. This can be obtained by some previous synchronization algorithms such as the method presented in [16].

A5: The channel can be considered as time-invariant because the characteristics of the channel vary very slowly with time [6], [16], [21] in an outdoor environment.

Note that in practical wireless networks, the interferences to the transmitter are existed and can not be ignored. However, for a transmitter equipped with an antenna array, there will be a trade-off between the mainlobe and the sidelobe of the beam pattern. This means that if the beam pattern has a low sidelobe, the interference of the transmitted signal will be reduced so that the power of the signal can focus on the mainlobe. The goal of this work is to find a method to optimize the VNAA so that the transmitter is able to generate a better signal with a high directivity of the mainlobe and a

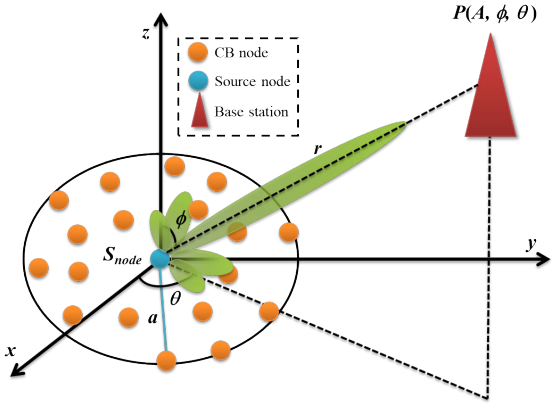

FIGURE 1. Geometrical configuration of CB based on the VNAA.

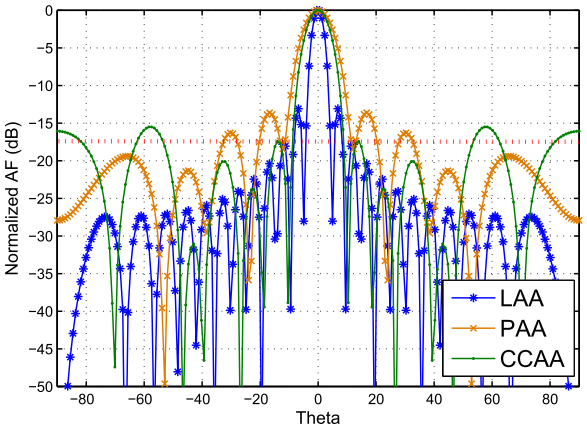

FIGURE 2. Beam patterns of the LAA, PAA and CCAA with the same number of elements.

low sidelobe toward the receiver. Therefore, no matter what kind of channel it uses or what kind of interference it is, the received signal noise ratio (SNR) will be improved if the sidelobe can be effectively reduced.

B. CB MODEL

Fig. 1 shows the sketch map of the distributed CB based on a VNAA. The elevation angle is denoted as $\theta \in [0, \pi]$, whereas the azimuth angle is denoted as $\phi \in [-\pi, \pi]$. We assume that the position of the target BS is (A, ϕ_0, θ_0) in a spherical coordinate system and it can be set up in a way so that $\phi_0 = 0$ and $\theta_0 = 0$. According to the electromagnetic wave superposition principle, the array factor (AF) can be approximated as follows [13]:

$$AF(\phi, \theta, \omega) = \sum_{k=1}^{N_{CB}} \omega_k e^{j\Psi_k} e^{j\frac{2\pi}{\lambda} d_k(\phi,\theta)} \tag{1}$$

where N_{CB} represents the number of sensor nodes, λ is the wavelength, ω_k is the amplitude weight, and Ψ_k is the initial phase of the kth node. Ψ_k is expressed as follows:

$$\Psi_k = -\frac{2\pi}{\lambda} d_k(\phi_0, \theta_0) \tag{2}$$

where d_k is the Euclidean metric between the kth sensor node and the target BS. The expression of d_k is as follows:

$$d_k = \sqrt{A^2 + r_k^2 - 2r_k A \sin(\theta)\cos(\phi - \psi_k)} \tag{3}$$

where r_k and ψ_k are the polar form coordinates of the kth node.

C. ENERGY CONSUMPTION MODEL

The following widely used energy consumption model in WSN is adopted in this study [6], [15]:

$$E_T = bE_{elec} + b\varepsilon_{fs} l^2 \tag{4}$$

$$E_R = bE_{elec} \tag{5}$$

where E_T and E_R represent the transmit and the receive energy consumptions of the nodes, respectively. E_{elec} is the electronic energy and it depends on several specific factors, for example, the digital coding method, b is the bit number, ε_{fs} is the amplifier energy and it is usually affected by the required sensitivity and the noise figure of the receiver, respectively. l is the distance between the transmitter and the receiver.

III. JOINT SIDELOBE SUPPRESSION APPROACH

A. ARRAY NODE LOCATION OPTIMIZATION

In typical WSNs, the positions of the nodes cannot move after they have been deployed. However, selecting the sensor nodes that are in the better positions from a large number of candidate nodes to form a VNAA can reduce the maximum SLL. In VNAA, an array node influences not only the EM field generated by its own amplitude but also by other nodes. If the distance between the elements is small, the electromagnetic coupling effects become greater, thereby causing the shifted of the mainlobe and the increasing of the maximum SLL [29]. In addition, the shapes of the antenna array also affect the maximum SLL, and the maximum SLL generated by a regularly-shaped antenna array is lower than that of an VNAA with the same number of array elements. Thus, we can first choose a group of array nodes based on a certain fixed shape in large numbers of randomly distributed array elements to avoid the EM coupling as far as possible, and then suppress the maximum SLL by further optimizing the amplitude weights of the selected array nodes.

Fig. 2 shows the 2D beam patterns of the linear antenna array (LAA), the planar antenna array (PAA) and the CCAA obtained with the same number of the array elements. It can be seen from the figure that the CCAA has better sidelobe performance than LAA and PAA. Thus, the CCAA can be used as the guide array during the node selection optimization process for CB. In addition, the communication coverage of a node is usually a circular area in wireless communications. Thus, the node selection method of VNAA based on CCAA is more in accordance with the law and it is convenient to dispatch.

Ideal Node ID	Nearest Candidate node ID (Increment by distance)
1	Node 3, Node 5, Node 2, Node 19…
2	Node 8, Node 4, Node 13, Node 1…
…	…
N	Node 2, Node 1, Node 12, Node 7…

FIGURE 3. Mapping table created by S_{node}.

Distributed CB can be divided into two main stages: data sharing and beamforming. Thus, the node selection strategy of the location optimization in CB mainly consists of the following steps:

Step 1: In the data sharing stage, the source node S_{node} calculates the element positions of the ideal CCAA according to the required node number N_{CB}. Then, the selection control message $M_{\text{selection}}$ that includes the positions of the ideal antenna elements is broadcasted in the range of R_{c} to all nodes in the CB cluster.

Step 2: All candidate nodes in the cluster receive $M_{\text{selection}}$, and calculate the distances between themselves and all ideal positions. After the calculation, all candidate nodes will return a feedback message M_{response} that includes the ID of their nearest ideal nodes, the distances between themselves and their nearest ideal nodes, their own coordinates, and the candidate node ID to S_{node}.

Step 3: S_{node} receives M_{response} returned by the candidate nodes. Then, S_{node} should select a set of array nodes that best meet the optimized condition based on the content in M_{feedback}. The selection process is detailed as follows.

First, S_{node} needs to create a simple mapping table between the ideal nodes and the candidate nodes according to M_{response}. The sketch map is shown in Fig. 3. It can be seen from the mapping table that each ideal position will have a most suitable corresponding candidate node that with the nearest distance from the ideal positions.

Second, S_{node} determines the array nodes from the mapping table. Obviously, the nodes with the nearest distances from the ideal locations will selected as the array nodes (which are the nodes marked red in Fig. 3).

Third, S_{node} determines the optimal amplitude weight of each selected array node by using the optimization method proposed in the next section.

Step 4: S_{node} broadcasts the beamforming message $M_{\text{beamforming}}$ mainly includes the selected array node ID, the information that needs to be sent to the BS, and the CB time, only to the selected array nodes.

Step 5: The selected array nodes use CB to send information to the BS, according to the CB time received in $M_{\text{beamforming}}$.

B. TRANSMISSION POWER OPTIMIZATION

To further optimize the performance of the beam pattern for CB, the amplitude of the selected array nodes needs to be optimized.

1) PROBLEM FORMULATION

To jointly reduce the maximum SLL of the beam pattern and the amplitude so that saving energy, the following optimization problem can be formulated:

$$\min \quad \alpha \cdot \left| \frac{\max |AF(\theta_{\text{SL}})|}{AF(\theta_{\text{ML}})} \right| + \beta \cdot \sum_{k=1}^{N_{CB}} \omega_k \tag{6a}$$

$$\text{s.t.} \quad 0 \leqslant \omega_i \leqslant 1, \quad \forall i \in N_{CB} \tag{6b}$$

$$\theta_{\text{ML}} = \arg(\max |AF(\theta)|), \quad \theta \in [-\pi, \pi] \tag{6c}$$

$$\text{s.t.} \quad \theta_{\text{SL}} \in [-\pi, \theta_{\text{FN1}}) \cup (\theta_{\text{FN2}}, \pi] \tag{6d}$$

$$\text{s.t.} \quad SNR \geqslant \eta_{thr} \tag{6e}$$

where θ_{SL} and θ_{ML} represent the positions of the sidelobe and the mainlobe, respectively, during the optimization process. θ_{FN1} and θ_{FN2} are the two first nulls around the mainlobe. α and β are the weight factors that can balance the optimization between the SLL and the amplitude weight, $\alpha + \beta = 1$. The main purpose of our work is to reduce the maximum SLL. Thus, we choose $\alpha = 0.7$ and $\beta = 0.3$, respectively [30]. Moreover, SNR is the signal-to-noise ratio (SNR) at the receiver (e.g., intended BS), and it should be larger than a threshold η_{thr} to guarantee that the amplitude weight optimization does not cause the transmission to fall below the required signal level. In the optimization process, the SNR constraint will be handled by the widely used stochastic ranking technique [31]. The goal of the formulated optimization problem is to find a set of minimum amplitude weights ω of a VNAA that can achieve a minimized maximum SLL.

The formulated optimization problem in Eq. (6) is NP-hard and the proof is as follows.

Proof: For ease of analysis, the formulated continuous optimization problem is first converted to a discrete form (which means the solution can be only chosen as several fixed values from 0 or 1), as follows:

$$\min \quad \alpha \cdot \left| \frac{\max |AF(\theta_{\text{SL}})|}{AF(\theta_{\text{ML}})} \right| + \beta \cdot \sum_{k=1}^{N_{CB}} \hat{\omega}_k \tag{7a}$$

$$\text{s.t.} \quad \hat{\omega}_i \in \Omega, \quad \forall i \in N_{CB} \tag{7b}$$

$$\theta_{\text{ML}} = \arg(\max |AF(\theta)|), \quad \theta \in [-\pi, \pi] \tag{7c}$$

$$\theta_{\text{SL}} \in [-\pi, \theta_{\text{FN1}}) \cup (\theta_{\text{FN2}}, \pi] \tag{7d}$$

$$SNR \geqslant \eta_{thr} \tag{7e}$$

where $\Omega \in \{0.1, 0.2, 0.3, \ldots, 1.0\}$ is a set with finite numbers of elements. Then, we will verify that the converted optimization problem shown in Eq. (7) is a combinatorial optimization problem (COP).

A COP can be represented by the following three factors that are (F, G, D) [32], where F is the cost function (Eq. (7a)), G represents the feasible solution region, and it is a set of constraint functions (Eq. (7b)), and D is the domain of solutions (Eqs. (7c)-(7d)). Thus, the converted optimization problem can be regarded as a COP, which is NP-hard [33]. The converted optimization problem in Eq. (7) is one of the situations of the original optimization problem formulated in Eq. (6), and hence the problem in Eq. (6) is NP-hard. ■

2) CSO

Swarm intelligence optimization algorithms are the effective methods to solve the NP-hard problems. CSO [34] is one of the these algorithms and it is based on three basic rules:

(1) The chickens are usually divided into different groups. In Each group, there are a dominant rooster and a couple of hens and chicks with mother-child relationships. A competitive relationship exists between each group.
(2) The fitness values determine the identities of the chickens including rooster, hens and chicks. Specifically, the chicken with several best fitness values can be regarded as the roosters, the chicken with several worst fitness values are defined as the chicks, and other chicken are the hens. Moreover, the mother-child relationship between the hens and the chicks is randomly established. In addition, competition occurs among individuals in the foraging process, and the dominant individuals could snatch food foraged by other individuals.
(3) The hens need to follow the rooster in the same group to forage for food within a certain range, whereas the chicks search for food around their mother. Obviously, the dominant individuals have the advantages in competing for getting food.

In CSO, different position update methods are used for the individuals with different identities, and the dominant individuals have the advantage compared with other individuals. To achieve this case, we can simulate that the roosters can forage for food in a wider area. Thus, the position update method of the roosters can be formulated as follows:

$$x_{i,j}^{t+1} = x_{i,j}^{t} \cdot (1 + Gauss(0, \sigma^2)) \tag{8}$$

where $x_{i,j}^{t}$ represents the individual position at tth iteration, $Gauss(0, \sigma^2)$ is a Gaussian distribution with mean zero and standard deviation σ^2.

For the hens, they should follow the group mate roosters to find food. Moreover, they need to snatch better food foraged by other individuals. This phenomenon can be simulated by:

$$\begin{aligned} x_{i,j}^{t+1} = x_{i,j}^{t} &+ \exp\frac{f_i - f_{ri}}{(\mathrm{abs}(f_i) + \varepsilon)} \cdot Rand \cdot (x_{r1,j}^{t} - x_{i,j}^{t}) \\ &+ \exp(f_{r2} - f_{r1}) \cdot Rand \cdot (x_{r2,j}^{t} - x_{i,j}^{t}) \end{aligned} \tag{9}$$

where f is the fitness value, $Rand$ is a random number between 0 and 1. $r1 \in [1, \ldots, N]$ is the rooster index, whereas $r2 \in [1, \ldots, N]$ is the chicken index and it is randomly selected from the swarm, $r1 \neq r2$. ε is the smallest constant in the computer, and it is adopted to avoid the zero-division-error.

For the chicks, they can only move around the hens, and this can be described as follows:

$$x_{i,j}^{t+1} = x_{i,j}^{t} + FL \cdot (x_{m,j}^{t} - x_{i,j}^{t}) \tag{10}$$

where $x_{m,j}^{t}$ stands for the position of the ith hen, FL is used to represent that the chicks follow their mother to search for food. Given the differences among individuals, FL of each chick would be randomly chosen between 0 and 2.

3) LOCATION LEARNING MECHANISM

CSO is able to improve the convergence rate effectively through different location update mechanisms. To further improve the performance and make it applicable to optimize the amplitude weights for distributed CB, the position learning mechanism of the PSO algorithm is introduced to obtain an improved solution by learning the history solution. A historical update position mainly includes the local optimal and the global optimal solutions. The position update method by introducing the learning mechanism can be expressed as:

$$\begin{aligned} y_{i,j}^{t} = &\ Factor_1 \cdot Rand \cdot (pBestx^{t-1} - x_{i,j}^{t}) \\ &+ Factor_2 \cdot Rand \cdot (gBestx - x_{i,j}^{t}) \end{aligned} \tag{11}$$

$$x_{i,j}^{t+1} = x_{i,j}^{t} + y_{i,j}^{t} \tag{12}$$

where $Factor_1$ and $Factor_2$ are learning factors, $pBestx$ is the local optimal solution, and $gBestx$ is the global optimal solution.

This mechanism is used when the newly generated solution is worse than the previous one. For example, for a minimization optimization problem, if $f(x_t) < f(x_{t+1})$, then we say that the newly generated solution x_{t+1} is worse compared to x_t. At this time, the proposed location learning mechanism is adopted to improve the solution quality.

4) VARIATION MECHANISM

Historical record of the global best solution may introduce a tenacity towards premature convergence, which reduces the performance of the algorithm. To overcome this shortcoming, the variation mechanism is used to change one of the value of the worst individual in the population, and eventually to form a new individual [24]. The variation operator may prevent the algorithm from converging into the local optima. If the algorithm is in a stagnant state, which means that the global optimal solution was kept for the same value after several iterations, the worst individual in the population is variated, and the variation operator is as follows:

$$x_{i,j}^{t} = L_{\mathrm{b}} + (U_{\mathrm{b}} - L_{\mathrm{b}}) \cdot \mathrm{rand}(1, num_{\mathrm{d}}) \tag{13}$$

where L_{b} and U_{b} are the minimum and maximum values of the solutions, respectively. num_{d} represents the dimension of the solution.

5) STEPS OF THE VPCSO FOR AMPLITUDE OPTIMIZATION IN JSSA

The steps of the proposed VPCSO algorithm with variation and location learning mechanisms are shown in Algorithm 1. Using VPCSO to obtain the optimal amplitude weight for each array node can be described as follows.

Step 1: Population Initialization and parameter settings. The source node initializes a population of N_{CB} chickens, each value of the chicken in the population means a amplitude weight ω_k. Then, setting the parameter values used in the algorithm. G is the updating time step of the hierarchy and mother-child relationship after the competition.

Algorithm 1 VPCSO

Input: A population of N_{pop} chickens
Output: Best solution x_{best}

Initialize the parameters;
Set the objective function $f(x)$, $x = (x_1, \ldots, x_n)^T$;
Calculate the objective function values of the N_{pop} chickens;
while $t < t_{max}$ **do**
  if $t\%G = 0$ **then**
    Establish a hierarchal order in the population according to the values of objective functions;
    Divide the population into different groups;
    Determine the relationship between mother hens and the chicks in each group;
  end
  for $i = 1$ *to* N_{pop} **do**
    if $i = Index_{rooster}$ **then**
      Use Eqs. (8) to update;
    end
    if $i = Index_{hen}$ **then**
      Use Eqs. (9) to update;
    end
    if $i = Index_{chick}$ **then**
      Use Eqs. (10) to update;
    end
    Evaluate the new generated solution;
    if *the new generated solution is worse than the previous one* **then**
      Update the new solution using learning history update location (Eqs. (11) and (12));
    end
  end
  if *the number of the global optimal solution is kept for the same value during several iterations* **then**
    Variate the solution by Eq. (13);
  end
  Keep the best solution x_{best};
end
return x_{best};

Step 2: Fitness value evaluation. S_{node} should evaluate the population by using the fitness function described in Eq. (6a), then rank the fitness values of the chickens and establish a hierarchal order in the swarm.

Step 3: Solution updating.

Sub-step 3.1: S_{node} updates the solution using different equations described in Eqs. (8)-(13) according to the corresponding identities of the solutions. Then, S_{node} evaluates the new solutions.

Sub-step 3.2: If the new generated solution is better than the previous one, then update it. While if the new solution is worse than the previous one, the source node needs to update the new solution by the location learning mechanism.

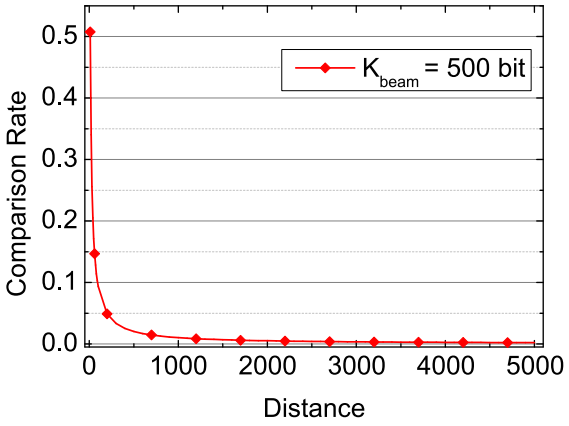

FIGURE 4. Energy overhead in the node selection stage.

Step 4: Variation operation. If the number of the global solution is kept for the same value during several iterations, the algorithm may fall into local optima. Hence, the source node should use the variation mechanism shown in Eq. (13) to update the solutions.

Step 5: End check. If the maximum iteration t_{max} arrives, the algorithm should stop. However, if the expected solutions are not obtained, the source node should go back to step 2 for a loop.

C. ENERGY CONSUMPTION ANALYSIS OF JSSA

According to the energy consumption model presented in section II-C, the energy overhead of the node selection method in JSSA mainly include four parts:

Part 1: S_{node} broadcasts a message M_{select} for initializing the node selection process. The energy consumption is:

$$E_{\text{con\_1}} = E_{\text{T\_source}} + N_{\text{candi}} \cdot E_{\text{R\_candi}} \tag{14}$$

Part 2: All the candidate nodes receives M_{select} and respond the feedback message M_{feedback} to S_{node}. The energy consumption of this process is:

$$E_{\text{con\_2}} = N_{\text{candi}} \cdot E_{\text{T\_candi}} + E_{\text{R\_source}} \tag{15}$$

Part 3: S_{node} broadcasts CB message M_{beam} to the selected CB array nodes. The energy consumption of this part is:

$$E_{\text{con\_3}} = E_{\text{T\_source}} + N_{\text{CB}} \cdot E_{\text{R\_CB}} \tag{16}$$

Part 4: The CB node array utilizes CB for data transmission. The energy consumption of this part is:

$$E_{\text{con\_4}} = N_{\text{CB}} \cdot E_{\text{beamforming}} \tag{17}$$

We define $E_{\text{selection}}$ as the energy consumption of the node selection stage, and define E_{total} as the total energy consumption of a whole CB process. Moreover, we set a ratio $\rho = \frac{E_{\text{selection}}}{E_{\text{total}}}$. For simplification, the distance between each CB array nodes and S_{node} is set as R_{c}. Thus, ρ can be extended to Eq. (18), as shown at the bottom of the next page. In this equation, N_{candi} is the number of the candidate nodes, N_{CB} is the number of the selected CB array nodes, k_{s} is the bit

length of the control message, and k_{beam} is the bit length of the data that need to be transmitted. We suppose $k_s = 50$ bit, $k_{\text{beam}} = 500$ bit, $N_{\text{candi}} = 100$, $N_{\text{CB}} = 10$, $R_c = 10$ m. Fig. 4 shows the change of ρ with the distance between the BS and the CB array. As can be seen, when the BS is located far away from a CB array, the value of ρ is small, which indicates that the control overhead of the CB process can even be disregarded. However, the control overhead becomes larger when the distance between the CB array and the BS is close. Therefore, CB is not applicable in small scale WSNs.

IV. SIMULATIONS AND ANALYSIS

In this section, the proposed JSSA is simulated by Matlab. The hardware platform used for the simulation is a desktop, the CPU is CORE i5 and the RAM is 4G. Moreover, the operating system of this computer is Window 10. The simulation is set as the single BS network scenario, and the beam patterns of the VNAA obtained by JSSA are first compared to the beam patterns obtained by the randomly selected nodes. Then, to evaluate the performance of the proposed VPCSO algorithm, the beam patterns obtained by VPCSO are compared to those obtained by other optimization algorithms. In addition, the performance of the proposed VPCSO are analyzed. Finally, EM simulations are conducted to verify the performance of the proposed JSSA in approximate practical real world applications.

A. PARAMETER TUNING AND SETUPS

The parameter settings of a nature-inspired algorithm for different problems are markedly different because different optimization problems have various characteristics. Thus, selecting a set of better parameters of the proposed VPCSO is necessary to achieve a better performance. In our simulations, the introduced learning factors which are $Factor_1$ and $Factor_2$ are changed during the tuning process to determine their optimal values in VPCSO. It can be seen from Fig. 5 that the optimal values of $Factor_1$ and $Factor_2$ are 0.8 and 3, respectively.

Moreover, the population size N_{pop} is also a pivotal parameter for an swarm intelligence algorithm. Although larger population size may improve the accuracy of the solution, this may also increase the overhead of the algorithm. Thus, N_{pop} should be determined. In this work, we changed the population sizes from 10 to 50 to determine which one is better for solving the CB optimization problem, and the results are shown in Fig. 6. As can be seen, the population size of 50 achieves a little bit better result, but it increases

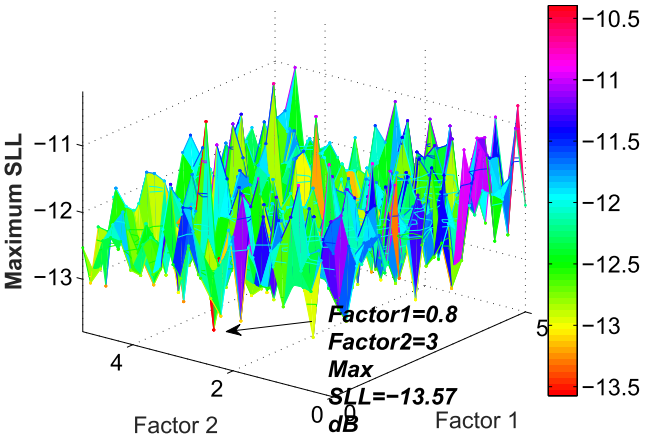

FIGURE 5. Parameter tunings for $Factor_1$ and $Factor_2$.

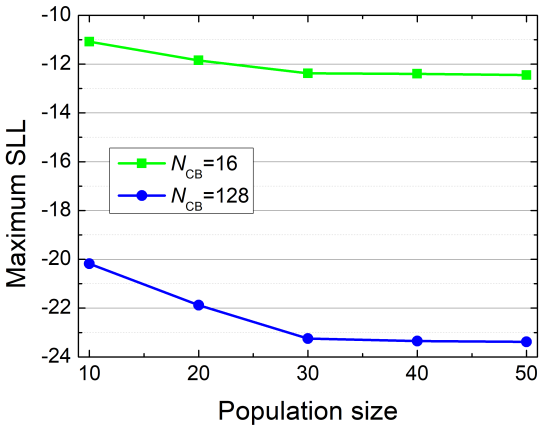

FIGURE 6. Parameter selections of population sizes of VPCSO for $N_{CB} = 16$ and $N_{CB} = 128$.

the computing overhead of the algorithm, which may be not suitable for the nodes with limited hardware resources in WSNs. In addition, the population size of 30 is widely used in many swarm intelligence algorithms since it has been demonstrated that this size can achieve an acceptable results of the problem [35]. Therefore, we use $N_{pop} = 30$ in this paper.

In this paper, BBO, CSO and PSO are selected as the comparison algorithms. Moreover, a new civilized swarm optimization with variation (CiSOV) algorithm which combines civilized swarm optimization [36] and the proposed variation mechanism is adopted to test if the variation mechanism is useful to deal with the global optimal trap. The key

$$\rho = \frac{E_{\text{selection\_stage}}}{E_{\text{selection\_stage}} + E_{\text{beam\_stage}}} = \frac{E_{\text{con\_1}} + E_{\text{con\_2}} + E_{\text{con\_3}}}{E_{\text{con\_1}} + E_{\text{con\_2}} + E_{\text{con\_3}} + E_{\text{con\_4}}}$$
$$= \frac{k_s E_{\text{elec}}(2N_{\text{candi}} + N_{\text{CB}} + 3) + k_s \varepsilon_{\text{fs}} R_c^2 (N_{\text{candi}} + 2)}{k_s E_{\text{elec}}(2N_{\text{candi}} + N_{\text{CB}} + 3) + k_s \varepsilon_{\text{fs}} R_c^2 (N_{\text{candi}} + 2) + k_{\text{beam}} N_{\text{CB}} E_{\text{elec}} + N_{\text{CB}}(\frac{k_{\text{beam}} \varepsilon_{\text{fs}} d_t^2}{N_{\text{CB}}^2})} \tag{18}$$

TABLE 1. Parameter settings of different algorithms.

Algorithm	Values of the parameters
BBO	$P_{modify} = 1, I = 1, E = 1$
CSO	$RN = 0.2 * N, HN = 0.6 * N, CN = N - RN - HN$
	$MN = 0.1 * N, G = 10, FL \in [0.5, 0.9]$
PSO	$c1 = 2, c2 = 2.5, w = 1$
CiSOV	$N_s = 4, w_{max} = 0.9, w_{min} = 0.4$
	$C_L = 2, C_{SL1} = 0.5, C_{SL2} = 1.5$
	$C_{SM1} = 0.25, C_{SM2} = 0.75$
VPCSO	$RN = 0.2 * N, HN = 0.6 * N, CN = N - RN - HN$
	$MN = 0.1 * N, G = 10, FL \in [0.5, 0.9]$
	$Factor_1 = 0.8, Factor_2 = 3$

parameter selections of these comparison approaches are listed in Table 1. P_{modify}, I, and E mean habitat modification probability, maximum immigration rate, and maximum emigration rate in BBO algorithm, respectively. c_1, c_2 and w indicate the learning factors and weighted factors in PSO. RN, HN, CN and MN represent the number of the roosters, the hens, the chicks and the mother hens in conventional CSO and VPCSO, respectively. The ratio of roosters, hens and chicks are suggested by [34] since this work verifies that this ratio achieves better results for most optimization problems. For CiSOV, N_s is the number of societies, w_{max} and w_{min} represent the inertia weight, and C_L, C_{SL1}, C_{SL2}, C_{SM1} and C_{SM2} are acceleration coefficients. In addition, we set the iterations of all the algorithms as 200 for the sake of fairness.

B. VERIFICATION OF THE IMPROVED FACTORS IN VPCSO

A test is conducted to verify the effectiveness of the introduced improved factors in VPCSO. In this test, the beam patterns of the 16-node CB array are optimized by using CSO, variation-CSO (VCSO) and particle-CSO (PCSO), respectively. Each optimization approach is run independently for 100 times and the average convergence rates during the optimization process are presented in Fig. 7. As can be seen, the introduced location learning mechanism is able to improve solution accuracy of the conventional CSO algorithm. This is because that the location learning mechanism can use globe optimal solution to guide the searching direction. Moreover, it also can be seen from Fig. 7 that the variation mechanism can effectively improve the convergence rate because if the global optimal solution is kept for the same value after several iterations, the worst individual in the population will be variated. Therefore, by combining the location learning and variation factors, the proposed VPCSO has better performance in terms of both accuracy and convergence rate.

C. BEAM PATTERNS

As shown in Fig. 8, 128 nodes are randomly distributed in an area, and a BS is located far away from this area. The location of BS does not have an impact on the selection of nodes for constructing the CB array. This is because the constructed CB VNAA is actually a planar antenna array, thus the mainlobe of its beam pattern can point in any direction of the space by controlling the parameters. Therefore, if the location of BS is changed, the performed CB array only needs to change the

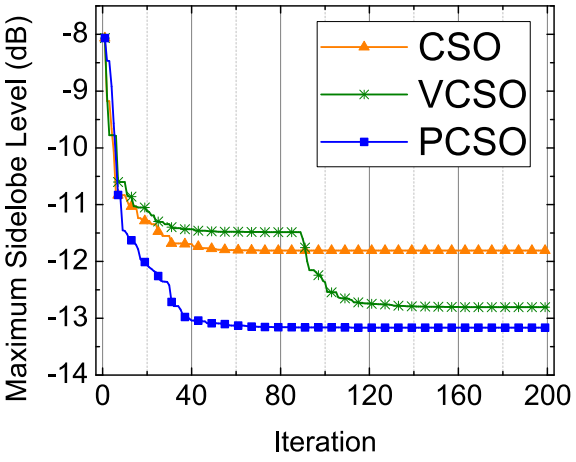

FIGURE 7. Verification of the improved factors in VPCSO.

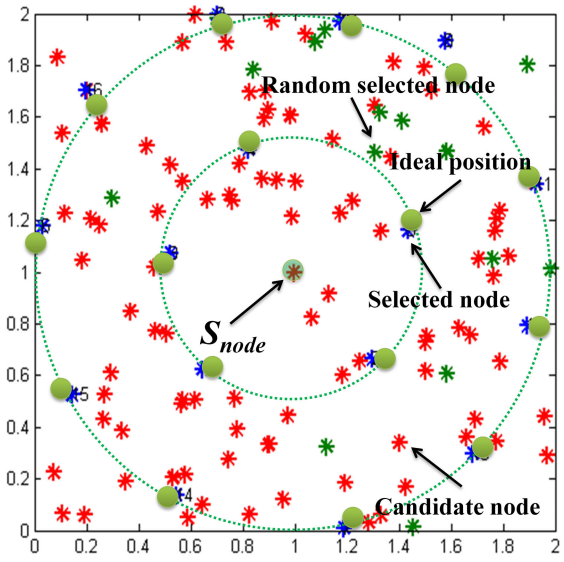

FIGURE 8. Node selection optimization results obtained by JSSA (select 16 array nodes from the total of 128 nodes).

direction of mainlobe to the direction of this BS. Moreover, the communication radius R_c is normalized to the wavelength and we assume $R_c = 1$ which refers to several previous works [25], [37]. Thus, the actual CB radius can be extended to other values by using different wavelengths in real-life applications. For example, if we use a signal with very high frequency (VHF), the wavelength will be 10 m to 1 m, and the CB ring radius will be 10 m to 1 m, which is practical for the outdoor environments.

In addition, in this simulation case, we assume 16 nodes need to be selected to form a VNAA for CB. The light green nodes in the figure are the array nodes selected by the proposed JSSA, the dark green nodes are the array nodes selected randomly, and the red nodes are the candidate nodes that have not been selected.

Then, we use the proposed VPCSO algorithm to further optimize the amplitude weights of 16 nodes selected by the

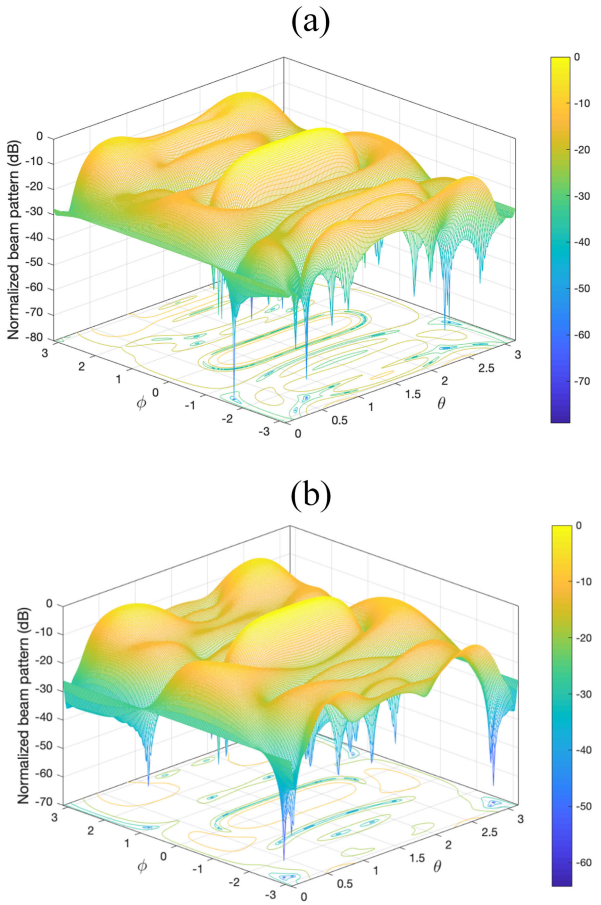

FIGURE 9. 3D beam patterns obtained by uniform amplitude weights and VPCSO $N_{CB} = 16$ and $R_c = 1$. (a) Uniform amplitude weights. (b) VPCSO.

position selection optimization process and compared its performance with that obtained by using other optimization algorithms. Fig. 9(a) and 9(b) show the three dimensional (3D) beam patterns obtained by the uniform amplitude weights and the proposed VPCSO, respectively, and Fig. 10 shows the two dimensional (2D) beam patterns of the CB array obtained by BBO, CSO, PSO, CiSOV and VPCSO. Note that the beam pattern optimizations are based on the entire three dimensional (3D) beam patterns [38], and here we show a selected 2D plane to show the results of different algorithms in a clearer way. In addition, the beam patterns without any optimizations and with only location optimization but without amplitude weight optimization are also shown in Fig. 10. The maximum SLL obtained by the proposed VPCSO is -13.8054 dB, and that by BBO, CSO, PSO and CiSOV are -12.7875 dB, -11.7754 dB, -11.1153 dB and -12.7634, and the maximum SLL is increased to -6.7680 dB and -8.2700 dB when obtained without any optimizations and with only location optimization, respectively. The maximum SLL obtained by only position optimization is lower than that without any optimizations. Moreover, VPCSO obtains the optimal SLL performance by further optimizing the amplitude weight, resulting in better results than that of all other optimization algorithms.

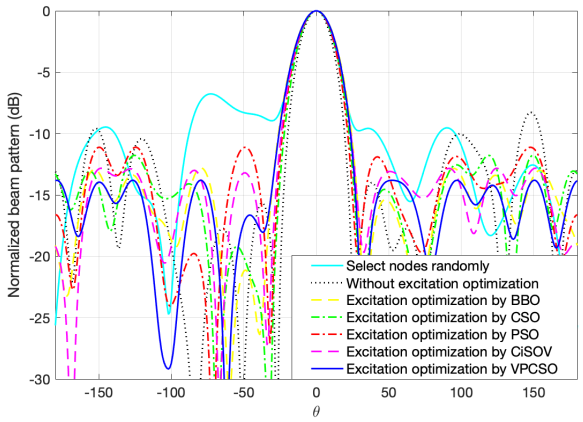

FIGURE 10. 2D beam patterns obtained by different algorithms for $N_{CB} = 16$ and $R_c = 1$.

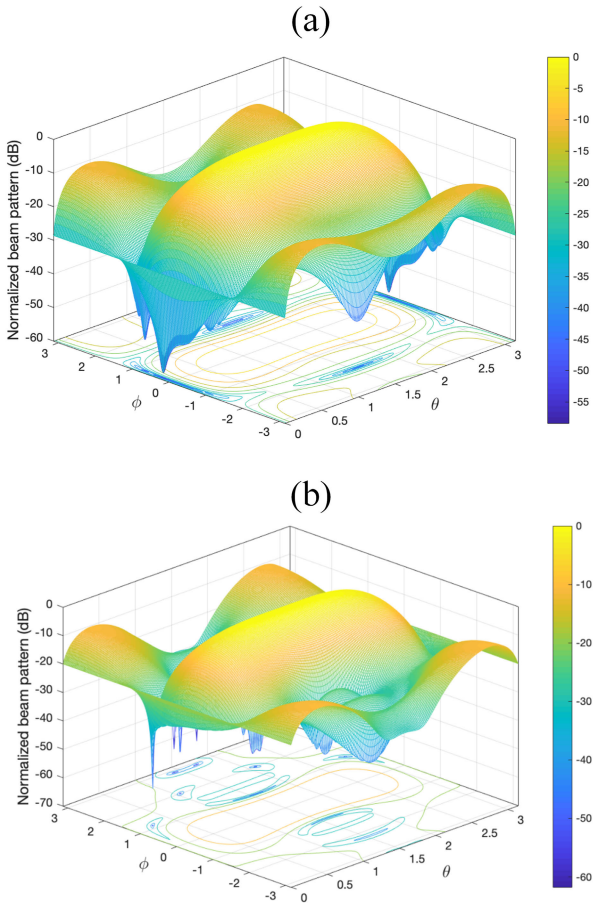

FIGURE 11. 3D beam patterns obtained by uniform amplitude weights and VPCSO $N_{CB} = 128$ and $R_c = 1$. (a) Uniform amplitude weights. (b) VPCSO.

To verify that VPCSO is able to maintain a better optimization performance when the number of nodes increases, which also leads to the increased solution dimensions, additional nodes are selected to form the VNAA. The chosen sample in Fig. 11 is one of the results obtained with $N_{CB} = 128$ and $R_c = 1$, and the corresponding 2D results are shown in Fig 12. Note that all the nodes in the area are selected if

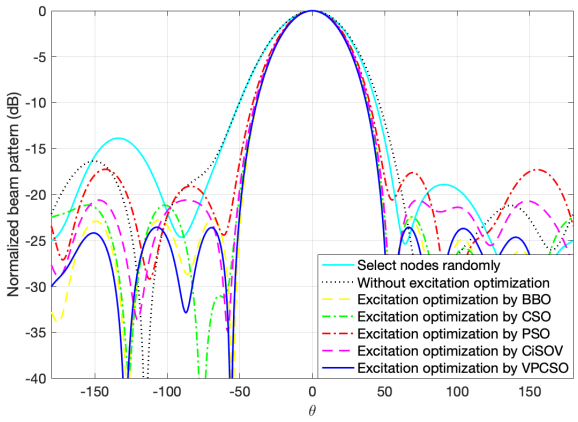

FIGURE 12. 2D beam patterns obtained by different algorithms for $N_{CB} = 128$ and $R_c = 1$.

the number of nodes increases to 128, and hence the problem of the node selection is not considered in this simulation. Moreover, Fig. 12 shows that the proposed VPCSO algorithm successfully reduces the maximum SLL of the beam pattern by approximately 7.1718 dB compared to the case without any optimizations, whereas the improvement by BBO, CSO, PSO and CiSOV are only 6.3103 dB, 4.8011 dB, 0.8999 dB and 4.7078 dB, respectively.

It also can be seen from these beam pattern figures that there are no grating lobes of the CB array. As we known, the grating lobe of a symmetrical antenna array will appear if the spacing between the elements is large than $\frac{\lambda}{2}$. However, it has been demonstrated that the grating lobe of a planar antenna array can be avoided by using the aperiodic arrays which means that allocating the antenna elements alternately [39]–[41]. This is also confirmed by [42], which uses genetic algorithm to add perturbations to the position of each element so that makes the array become aperiodic. Thus, the VNAA consists of sensor nodes may avoid grating lobes since the element placements are aperiodic naturally.

Fig. 13 shows the convergence rates of the five optimization algorithms. The proposed VPCSO algorithm has the highest solution accuracy and the fastest convergence rate compared to other algorithms in 16 node array. Moreover, we can see that although the number of the array nodes increases and it becomes a 128 node array, VPCSO also has a faster convergence rate and higher accuracy compared to the other algorithms. Therefore, VPCSO still has better optimization performance in large-scale CB optimization problems.

The distributions of the amplitude weights on the CB nodes obtained by different algorithms are shown in Fig. 14. The total amplitude weights of all the array nodes obtained by BBO, CSO, PSO, CiSOV are 8.9864, 8.3907, 12.6128 and 7.2368, whereas that obtained by VPCSO is 7.2125. In addition, the amplitude weight of each node is one for the conventional VNAA without any optimizations, and we define it as the uniform amplitude weights. Thus, the total amplitude weights obtained by the conventional beamforming method is 16. In summary, the total amplitude weights of CB nodes obtained by VPCSO decreased by 19.74%, 14.04%, 42.81%,

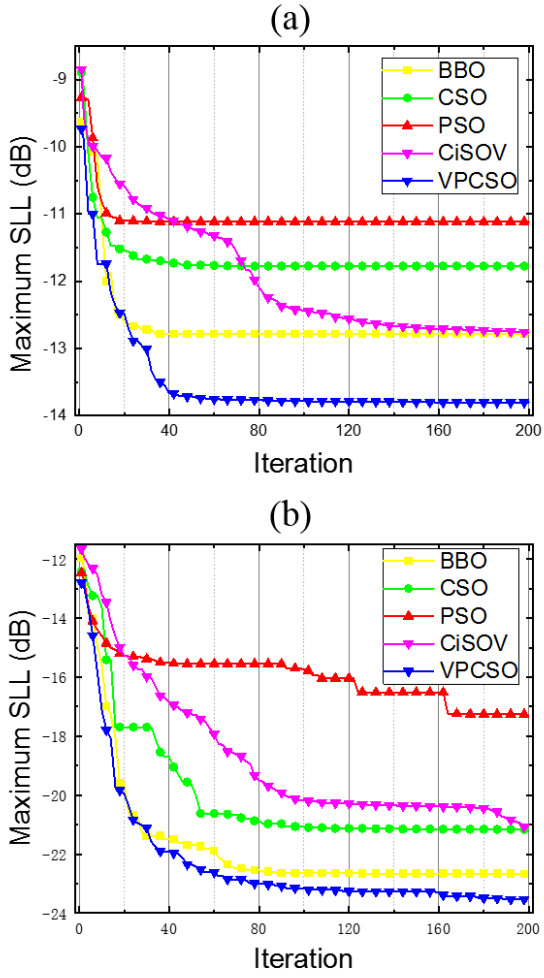

FIGURE 13. Convergence rates obtained by different algorithms. (a) $N_{CB} = 16$ and $R_c = 1$. (b) $N_{CB} = 128$ and $R_c = 1$.

54.78% and 54.92% compared with that obtained by BBO, CSO, PSO, CiSOV and the conventional method, respectively. Thus, VPCSO reduces the amplitude and energy consumption of the nodes.

D. PERFORMANCE ANALYSIS OF VPCSO

1) STABILITY VERIFICATION OF VPCSO

To verify the stability of VPCSO, 20 independent trials are run for optimizing the maximum SLL. Fig. 15 shows the trial results for $N_{CB} = 16$ and $N_{CB} = 128$, and Tables 2 and 3 show the numerical results of the best SLLs, the worst SLLs, the average values and the standard deviation (SD) obtained from the tests, for different values of N_{CB}, respectively. As can be seen from the table, the proposed VPCSO has the best accuracy performance as well as the stability. Moreover, the SD obtained by VPCSO for both cases are the lowest which indicates that it has the best stability.

2) INFLUENCES OF THE NUMBER OF THE NODES

Fig. 16 shows the maximum SLL of all the four optimization methods with different values of N_{CB}. It can be seen that the proposed VPCSO algorithm has a better optimization

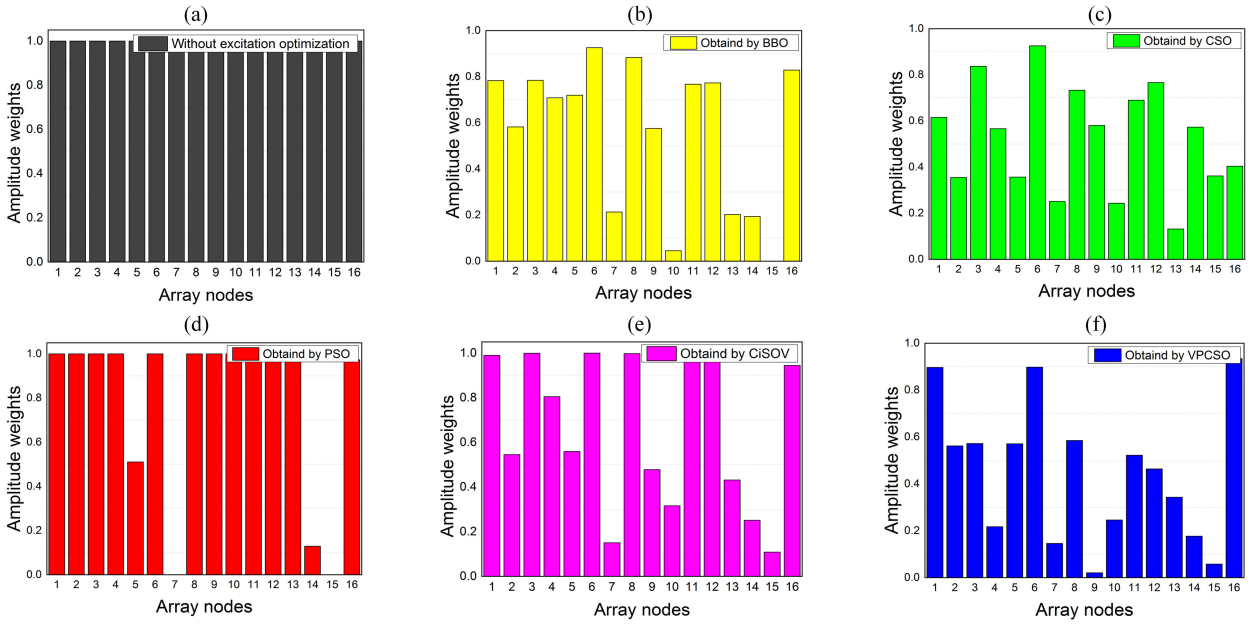

FIGURE 14. Amplitude weights of each array node obtained by different algorithms. (a) Uniform amplitude weights. (b) BBO. (c) CSO. (d) PSO. (e) CiSOV. (f) VPCSO.

TABLE 2. Statistical results of different algorithms ($K = 16$).

Algorithm	BBO	CSO	PSO	CiSOV	VPCSO
Best (dB)	-12.79	-11.78	-11.12	-12.76	-12.81
Worst (dB)	-10.16	-9.01	-9.09	-10.07	-12.01
Average (dB)	-11.19	-10.07	-9.98	-11.62	-12.35
SD (dB)	0.7394	0.7704	0.5694	0.6993	0.1656

TABLE 3. Statistical results of different algorithms ($K = 128$).

Algorithm	BBO	CSO	PSO	CiSOV	VPCSO
Best (dB)	-22.6	-21.61	-17.26	-21.10	-23.53
Worst (dB)	-19.16	-17.23	-15.91	-15.70	-22.98
Average (dB)	-21.16	-20.34	-16.57	-18.67	-23.21
SD (dB)	0.8315	0.9429	0.4625	1.4350	0.2643

effect than other algorithms with the increasing number of N_{CB}.

3) MAXIMUM SLLS RELATIVE TO DIFFERENT R_c

The maximum SLLs obtained by different optimization algorithms and communication radius are shown in Fig. 17. This figure shows that the proposed VPCSO algorithm has a better optimization result than other algorithms. However, the optimization effect decreases when the communication radius increases because that the mutual coupling affects the SLL of the VNAA if the average spacing between the array elements is less than 0.5 [29]. However, with the increasing of R_c, the spacing between the array nodes can be kept more than 0.5. Thus, the effect of mutual coupling can be reduced so that the SLL performances are better in larger R_c conditions naturally. For this reason, a higher improvement of the maximum SLL is achieved for smaller R_c.

4) 3 db BEAMWIDTH

Fig. 18 shows the 3 dB beamwidth of all the six methods with different values of R_c. If $R_c < 5$, the 3 dB beamwidth of the beam pattern obtained with only location optimization is the lowest, and the gap among other algorithms is not evident. However, if $R_c > 5$, different algorithms can almost achieve a similar 3 dB beamwidth. They are all higher than the beam patterns without any optimizations.

5) CCDF

The CCDF of the beam pattern is defined as the probability that the average transmit power at a certain direction θ exceeds a threshold power P_0. Thus, CCDF can be written as follows [30]:

$$CCDF = 20\log_{10}\left(\frac{AF(\theta,\omega)}{AF(\theta_{ML},\omega)}\right) > P, \quad \theta \in [-\pi,\pi] \quad (19)$$

The 3 dB beamwidth obtained by VPCSO is similar to that obtained by the other algorithms. The sidelobe range produced by VPCSO is larger than that of the beam patterns obtained without any optimizations. However, the proposed VPCSO algorithm achieves the better CCDF performance, as shown in Fig. 19. Thus, VPCSO still has a good direction performance.

6) ENERGY CONSUMPTION COMPARISON

Fig. 20 shows the average energy consumptions of the low energy adaptive clustering hierarchy (LEACH) [43], the hybrid, energy-efficient, distributed (HEED) clustering approach [44] and the proposed JSSA. The source node is about 1000 m away from the BS. It can be seen from the figure that the proposed JSSA has advantages in the average energy consumption compared to LEACH and HEED. This is because the BS can achieve an increase of N_{CB}^2 by using CB, and the power of each sensor node in the network will be reduced to $1/N_{CB}^2$. Thus, JSSA based on CB can save energy.

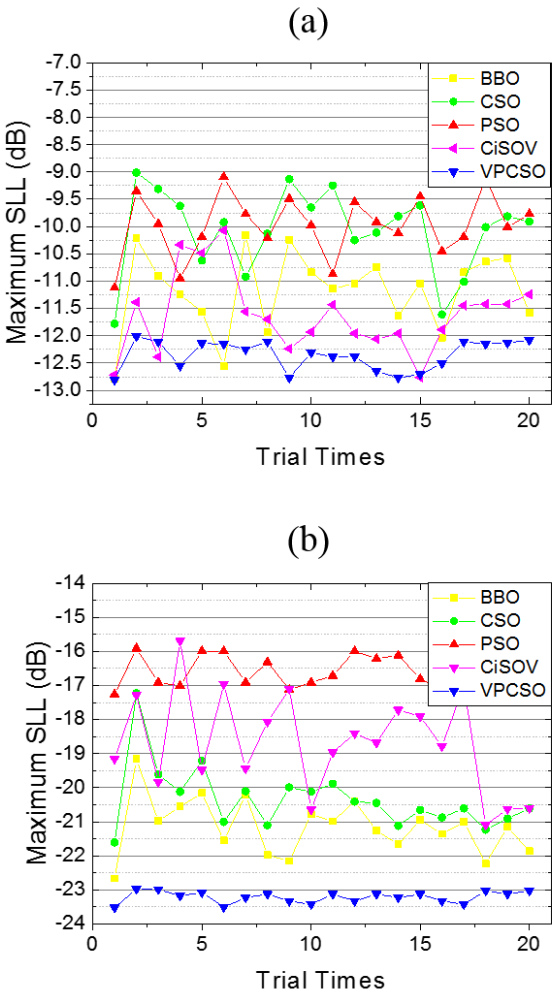

FIGURE 15. Maximum SLLs obtained from 20 independent trials. (a) $N_{CB} = 16$. (b) $N_{CB} = 128$.

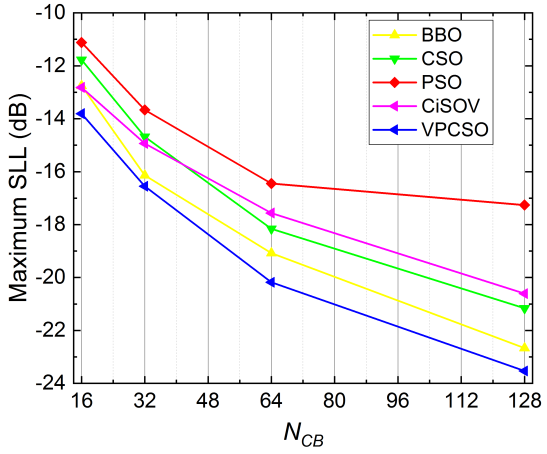

FIGURE 16. Comparisons of the maximum SLL and N_{CB} obtained by different algorithms.

However, Fig. 20 also indicates that the proposed JSSA consume more energy than other algorithms in the network initialization stage. The reason is that when the network is initializing, JSSA has to spend more energy for selecting the CB

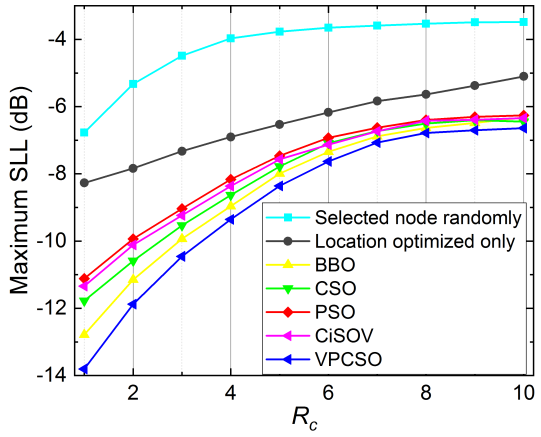

FIGURE 17. Comparisons of the maximum SLLs related to R_c obtained by different algorithms.

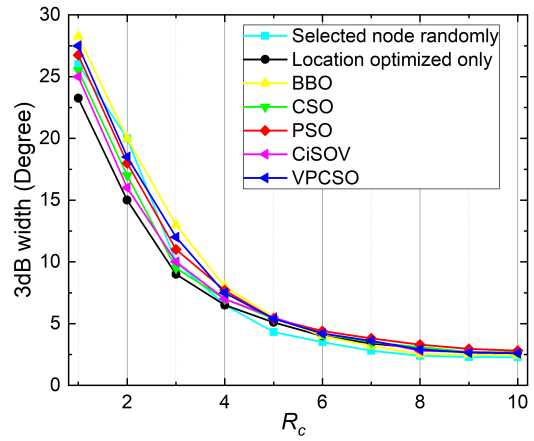

FIGURE 18. Comparisons of 3 dB beamwidth with the increasing of R_c.

array nodes and for the inner array communications. However, according to the analysis in section III-C, the energy consumption overhead of the node selection process can be basically disregarded compared to the energy consumption overhead of the CB stage.

E. EM SIMULATION

In this work, the mutual coupling between the antenna elements are ignored when formulating the maximum SLL suppression problem, as with the existing works on the beam pattern optimizations of CB. However, the effects of the mutual coupling exist in the real world applications. Thus, in this section, we conduct EM simulations based on ANSYS Electromagnetics 2016 (HFSS) to verify the beam pattern performances of the VNAAs obtained by different algorithms in the approximate EM environment. In this EM simulation, a VNAA is constructed and each element in the VNAA is designed with the same physical structure. Moreover, the number and the locations of the elements are the same with the simulation results obtained from Section IV-C (select 16 array nodes from the total of 128 nodes). For the amplitude, similar to [25], [45], the optimized amplitude weights

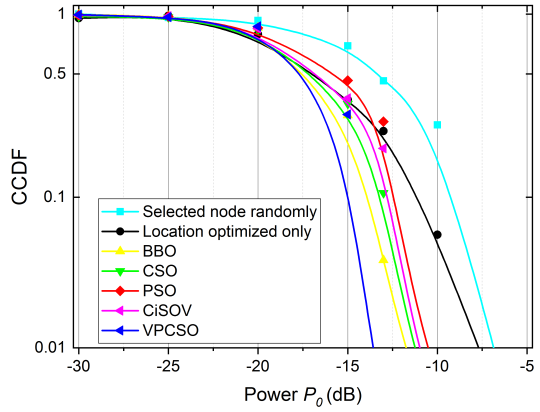

FIGURE 19. Comparisons of CCDF obtained by different algorithms.

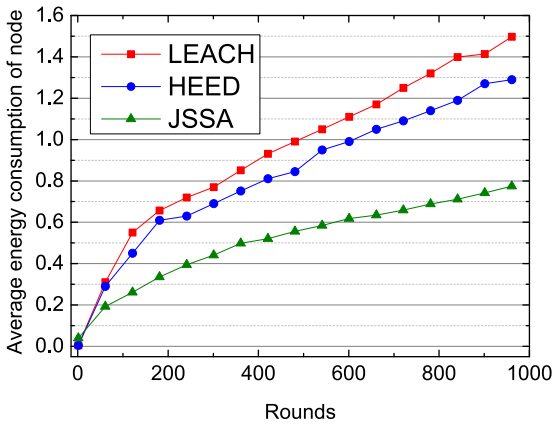

FIGURE 20. Average energy consumption of different approaches.

in ideal condition obtained by Matlab without considering the mutual coupling is plugged into HFSS, which can be regarded as a more practical environment, to evaluate that if the solution obtained by the ideal conditions is effective for the practical VNAA which considers the EM factors.

Fig. 21 shows the two-dimensional (2D) polar coordinate form beam patterns of the VNAA with the random selected nodes and the location optimized nodes, and the amplitude weights of these two VNAAs are both uniform. As can be seen, the mainlobe beamwidth of the VNAA with the random selected nodes is too wide. Thus, the beam pattern of the VNAA with the location optimized nodes is much better than that of the random selected nodes. Fig. 22 shows the 2D polar coordinate form beam patterns of the VNAA with different amplitude weights obtained by different algorithms including uniform, BBO, CSO, PSO, CiSOV and the proposed VPCSO, respectively. As can be seen, the maximum SLL obtained by VPCSO is the lowest among all the approaches. Therefore, similar to the simulations of the theoretical VNAA for CB, the proposed method can get a lower maximum SLL in practical environment, and hence, similar to the conclusion in [25], the beam pattern optimizations in an ideal condition are able to provide a general overview of the effectiveness of different optimization algorithms.

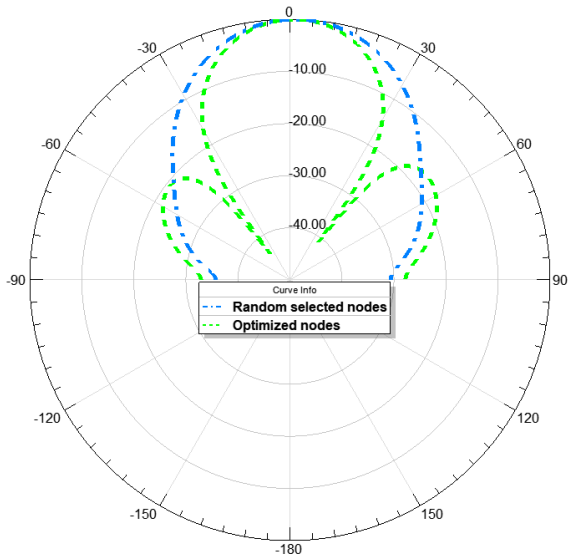

FIGURE 21. Beam patterns obtained by the random selected nodes and the location optimized nodes in EM simulation.

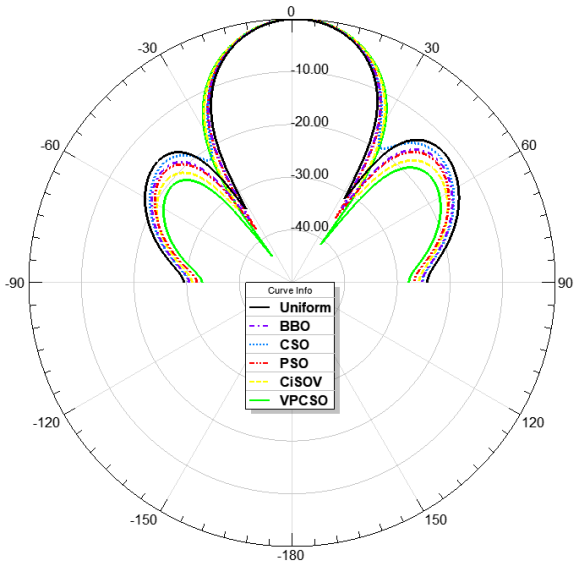

FIGURE 22. Beam patterns based on different amplitude weights obtained by different algorithms in EM simulation.

V. CONCLUSION

In this paper, a joint sidelobe reduction method called JSSA is proposed to suppress the maximum SLL of CB in WSNs. JSSA uses a node location optimization mechanism based on CCAA to compensate for the node position errors caused by the random distributions of the nodes. Then, the amplitude weights of the selected CB array nodes are further optimized by the proposed VPCSO algorithm. Simulation are conducted and the results show that the proposed location optimization method of JSSA can effectively reduce the maximum SLLs of the beam patterns compared to the conventional VNAA, and the amplitude weights optimized by VPCSO can further suppress the maximum SLL with various communication radii. The accuracy and the convergence rate of VPCSO are

better than those obtained by BBO, CSO, and PSO. Moreover, the energy-saving performance of VPCSO is better than those of the other algorithms, and several performance analysis tests show that the proposed VPCSO has the best performance. Finally, we conduct EM simulations to verify the performance of the proposed JSSA. The results show that JSSA may be also effect in practical real world applications.

ACKNOWLEDGMENT

A previous version of this paper is accepted for publication at the IEEE 90th Vehicular Technology Conference (VTC2019-Fall).

REFERENCES

[1] Q. Ju, G. Sun, H. Li, and Y. Zhang, "Collaborative in-network processing for Internet of battery-less things," *IEEE Internet Things J.*, vol. 6, no. 3, pp. 5184–5195, Jun. 2019.
[2] O. Kaiwartya, A. H. Abdullah, Y. Cao, J. Lloret, S. Kumar, R. R. Shah, M. Prasad, and S. Prakash, "Virtualization in wireless sensor networks: Fault tolerant embedding for Internet of Things," *IEEE Internet Things J.*, vol. 5, no. 2, pp. 571–580, Apr. 2018.
[3] T. O. Olasupo and C. E. Otero, "A framework for optimizing the deployment of wireless sensor networks," *IEEE Trans. Netw. Service Manage.*, vol. 15, no. 3, pp. 1105–1118, Sep. 2018.
[4] P. Kamalinejad, C. Mahapatra, Z. Sheng, S. Mirabbasi, V. C. M. Leung, and Y. L. Guan, "Wireless energy harvesting for the Internet of Things," *IEEE Commun. Mag.*, vol. 53, no. 6, pp. 102–108, Jun. 2015.
[5] W. Wei, H. Gu, K. Wang, X. Yu, and X. Liu, "Improving cloud-based IoT services through virtual network embedding in elastic optical inter-DC networks," *IEEE Internet Things J.*, vol. 6, no. 1, pp. 986–996, Feb. 2019.
[6] G. Sun, Y. Liu, A. Wang, J. Zhang, X. Zhou, and Z. Liu, "Sidelobe control by node selection algorithm based on virtual linear array for collaborative beamforming in WSNs," *Wireless Pers. Commun.*, vol. 90, no. 3, pp. 1443–1462, Oct. 2016.
[7] D. Wang, W. Li, and P. Wang, "Measuring two-factor authentication schemes for real-time data access in industrial wireless sensor networks," *IEEE Trans. Ind. Informat.*, vol. 14, no. 9, pp. 4081–4092, Sep. 2018.
[8] R. E. Mohamed, W. R. Ghanem, A. T. Khalil, M. Elhoseny, M. Sajjad, and M. A. Mohamed, "Energy efficient collaborative proactive routing protocol for wireless sensor network," *Comput. Netw.*, vol. 142, pp. 154–167, Sep. 2018.
[9] E. Alnawafa and I. Marghescu, "New energy efficient multi-hop routing techniques for wireless sensor networks: Static and dynamic techniques," *Sensors*, vol. 18, no. 6, p. 1863, Jun. 2018.
[10] G. Sun, Y. Liu, H. Li, A. Wang, S. Liang, and Y. Zhang, "A novel connectivity and coverage algorithm based on shortest path for wireless sensor networks," *Comput. Elect. Eng.*, vol. 71, pp. 1025–1039, Oct. 2018.
[11] Q. Ju, H. Li, and Y. Zhang, "Power management for kinetic energy harvesting IoT," *IEEE Sensors J.*, vol. 18, no. 10, pp. 4336–4345, May 2018.
[12] H. Jung and I.-H. Lee, "Secrecy performance analysis of analog cooperative beamforming in three-dimensional Gaussian distributed wireless sensor networks," *IEEE Trans. Wireless Commun.*, vol. 18, no. 3, pp. 1860–1873, Mar. 2019.
[13] H. Ochiai, P. Mitran, H. V. Poor, and V. Tarokh, "Collaborative beamforming for distributed wireless ad hoc sensor networks," *IEEE Trans. Signal Process.*, vol. 53, no. 11, pp. 4110–4124, Nov. 2005.
[14] S. Jayaprakasam, S. K. A. Rahim, and C. Y. Leow, "Distributed and collaborative beamforming in wireless sensor networks: Classifications, trends, and research directions," *IEEE Commun. Surveys Tuts.*, vol. 19, no. 4, pp. 2092–2116, 4th quart., 2017.
[15] G. Sun, Y. Liu, J. Zhang, A. Wang, and X. Zhou, "Node selection optimization for collaborative beamforming in wireless sensor networks," *Ad Hoc Netw.*, vol. 37, pp. 389–403, Feb. 2016.
[16] J.-C. Chen, C.-K. Wen, and K.-K. Wong, "An efficient sensor-node selection algorithm for sidelobe control in collaborative beamforming," *IEEE Trans. Veh. Technol.*, vol. 65, no. 8, pp. 5984–5994, Aug. 2016.
[17] S. Jayaprakasam, S. K. A. Rahim, and C. Y. Leow, "PSOGSA-Explore: A new hybrid metaheuristic approach for beampattern optimization in collaborative beamforming," *Appl. Soft Comput.*, vol. 30, pp. 229–237, May 2015.
[18] G. Sun, Y. Liu, Z. Chen, A. Wang, and Y. Zhang, "Radiation beam pattern synthesis of concentric circular antenna arrays using hybrid approach based on Cuckoo search," *IEEE Trans. Antennas Propag.*, vol. 66, no. 9, pp. 4563–4576, Sep. 2018.
[19] E. Tohidi, M. M. Nayebi, and H. Behroozi, "Dynamic programming applied to large circular arrays thinning," *IEEE Trans. Antennas Propag.*, vol. 66, no. 8, pp. 4025–4033, Aug. 2018.
[20] X. Zhang, D. Lu, X. Zhang, and Y. Wang, "Antenna array design by a contraction adaptive particle swarm optimization algorithm," *EURASIP J. Wireless Commun. Netw.*, vol. 2019, p. 57, Dec. 2019.
[21] M. F. A. Ahmed and S. A. Vorobyov, "Sidelobe control in collaborative beamforming via node selection," *IEEE Trans. Signal Process.*, vol. 58, no. 12, pp. 6168–6180, Dec. 2010.
[22] A. Chatterjee, G. K. Mahanti, and B. C. Mahato, "Sidelobe reduction of a scanned and broadside central element fed concentric ring array antenna with fixed first null beamwidth using novel particle swarm optimisation," *Int. J. Signal Imag. Syst. Eng.*, vol. 5, no. 4, pp. 290–294, 2012.
[23] N. Nik Abd Malik, M. Esa, S. S. Yusof, S. A. Hamzah, and M. K. H. Ismail, "Circular collaborative beamforming for improved radiation beampattern in WSN," *Int. J. Distrib. Sensor Netw.*, vol. 9, no. 7, Jul. 2013, Art. no. 125423.
[24] G. Ram, D. Mandal, R. Kar, and S. P. Ghoshal, "Pencil beam pattern synthesis of time-modulated concentric circular antenna array using pso with aging leader and challenger," *J. Electromagn. Waves Appl.*, vol. 29, no. 12, pp. 1610–1629, Jun. 2015.
[25] S. Jayaprakasam, S. K. A. Rahim, C. Y. Leow, T. O. Ting, and A. A. Eteng, "Multiobjective beampattern optimization in collaborative beamforming via NSGA-II with selective distance," *IEEE Trans. Antennas Propag.*, vol. 65, no. 5, pp. 2348–2357, May 2017.
[26] G. Ram, D. Mandal, R. Kar, and S. P. Ghoshal, "Optimized hyper beamforming of receiving linear antenna arrays using Firefly algorithm," *Int. J. Microw. Wireless Technol.*, vol. 6, no. 2, pp. 181–194, Apr. 2014.
[27] S. Liang, T. Feng, and G. Sun, "Sidelobe-level suppression for linear and circular antenna arrays via the cuckoo search–chicken swarm optimisation algorithm," *IET Microw., Antennas Propag.*, vol. 11, no. 2, pp. 209–218, Jan. 2017.
[28] A. Sharaqa and N. Dib, "Design of linear and elliptical antenna arrays using biogeography based optimization," *Arabian J. Sci. Eng.*, vol. 39, no. 4, pp. 2929–2939, Apr. 2014.
[29] V. Agrawal and Y. Lo, "Mutual coupling in phased arrays of randomly spaced antennas," *IEEE Trans. Antennas Propag.*, vol. AP-20, no. 3, pp. 288–295, May 1972.
[30] G. Sun, Y. Liu, J. Li, Y. Zhang, and A. Wang, "Sidelobe reduction of large-scale antenna array for 5G beamforming via hierarchical cuckoo search," *Electron. Lett.*, vol. 53, no. 16, pp. 1158–1160, Aug. 2017.
[31] T. P. Runarsson and X. Yao, "Stochastic ranking for constrained evolutionary optimization," *IEEE Trans. Evol. Comput.*, vol. 4, no. 3, pp. 284–294, Sep. 2000.
[32] C. Blum, J. Puchinger, G. R. Raidl, and A. Roli, "Hybrid metaheuristics in combinatorial optimization: A survey," *J. Appl. Soft Comput.*, vol. 11, no. 6, pp. 4135–4151, 2011.
[33] P. Belotti, C. Kirches, S. Leyffer, J. Linderoth, J. Luedtke, and A. Mahajan, "Mixed-integer nonlinear optimization," *Acta Numer.*, vol. 22, pp. 1–131, 2013.
[34] X. Meng, Y. Liu, X. Gao, and H. Zhang, "A new bio-inspired algorithm: Chicken swarm optimization," in *Proc. Int. Conf. Swarm Intell.* Hefei, China: Springer, 2014, pp. 86–94.
[35] K. Mistry, L. Zhang, S. C. Neoh, C. P. Lim, and B. Fielding, "A micro-GA embedded PSO feature selection approach to intelligent facial emotion recognition," *IEEE Trans. Cybern.*, vol. 47, no. 6, pp. 1496–1509, Jun. 2017.
[36] A. I. Selvakumar and K. Thanushkodi, "Optimization using civilized swarm: Solution to economic dispatch with multiple minima," *Electr. Power Syst. Res.*, vol. 79, no. 1, pp. 8–16, Jan. 2009.
[37] O. Ben Smida, S. Zaidi, S. Affes, and S. Valaee, "Robust distributed collaborative beamforming for wireless sensor networks with channel estimation impairments," *Sensors*, vol. 19, p. 1061, Mar. 2019.
[38] S. Das, R. Bera, D. Mandal, S. P. Ghoshal, and R. Kar, "Evolutionary algorithms based synthesis of low sidelobe hexagonal arrays," *Swarm Evol. Comput.*, vol. 38, pp. 139–157, Feb. 2018.
[39] T. Suda, T. Takano, and Y. Kazama, "Grating lobe suppression in an array antenna with element spacing greater than a half wavelength," in *Proc. IEEE Antennas Propag. Soc. Int. Symp.*, Jul. 2010, pp. 1–4.

[40] I. D. H. Sáenz, R. Guinvarc'h, R. L. Haupt, and K. Louertani, "A dual-polarized wideband planar phased array with spiral antennas," *IEEE Trans. Antennas Propag.*, vol. 62, no. 9, pp. 4547–4553, Sep. 2014.
[41] R. L. Haupt, "Optimized element spacing for low sidelobe concentric ring arrays," *IEEE Trans. Antennas Propag.*, vol. 56, no. 1, pp. 266–268, Jan. 2008.
[42] M. G. Bray, D. H. Werner, D. W. Boeringer, and D. W. Machuga, "Optimization of thinned aperiodic linear phased arrays using genetic algorithms to reduce grating lobes during scanning," *IEEE Trans. Antennas Propag.*, vol. 50, no. 12, pp. 1732–1742, Dec. 2002.
[43] W. B. Heinzelman, A. P. Chandrakasan, and H. Balakrishnan, "An application-specific protocol architecture for wireless microsensor networks," *IEEE Trans. Wireless Commun.*, vol. 1, no. 4, pp. 660–670, Oct. 2002.
[44] O. Younis and S. Fahmy, "HEED: A hybrid, energy-efficient, distributed clustering approach for ad hoc sensor networks," *IEEE Trans. Mobile Comput.*, vol. 3, no. 4, pp. 366–379, Oct./Dec. 2004.
[45] G. Sun, Y. Liu, H. Li, J. Li, A. Wang, and Y. Zhang, "Power-pattern synthesis for energy beamforming in wireless power transmission," *Neural Comput. Appl.*, vol. 30, no. 7, pp. 2327–2342, Oct. 2018.

SHUANG LIANG received the B.S. degree in communication engineering from Dalian Polytechnic University, China, in 2011, and the M.S. degree in software engineering from Jilin University, China, in 2017, where she is currently pursuing the Ph.D. degree in computer science. Her current research interests include wireless communication and design of array antennas.

ZHIYI FANG received the Ph.D. degree in computer science from Jilin University, Changchun, China, in 1998. He was a Senior Visiting Scholar with The University of Queensland, Australia, from 1995 to 1996, and with the University of California at Santa Barbara, Santa Barbara, CA, USA, from 2000 to 2001. He is currently a Professor in computer science with Jilin University. His current research interests include distributed/parallel computing systems, mobile communication, and wireless networks. He is a member of the China Software Industry Association and the Open System Committee of China Computer Federation.

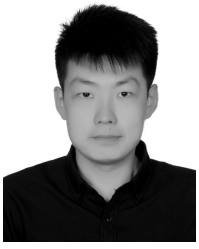

GENG SUN (S'17–M'18) received the B.S. degree in communication engineering from Dalian Polytechnic University, China, and the Ph.D. degree in computer science from Jilin University, China, in 2011 and 2018, respectively. He was a Visiting Researcher with the School of Electrical and Computer Engineering, Georgia Institute of Technology, USA. He is currently a Postdoctoral Researcher with the College of Computer Science and Technology, Jilin University. His current research interests include wireless sensor networks, antenna array, and collaborative beamforming and optimizations.

YANHENG LIU received the M.Sc. and Ph.D. degrees in computer science from Jilin University, China. He is currently a Professor with Jilin University. His current research interests include network security, network management, and mobile computing network theory and applications.

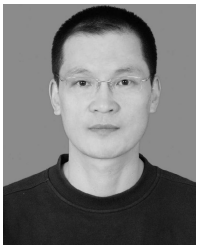

XIAOHUI ZHAO (M'14) received the bachelor's and master's degrees in electrical engineering from the Jilin University of Technology, Changchun, China, in 1982 and 1986, respectively, and the Ph.D. degree in control theory from the Universite de Technologie de Compiegne, Compiegne, France, in 1993. He is currently a Professor with the College of Communication Engineering, Jilin University, Changchun. He has authored or coauthored two books and various articles in the fields of cognitive radio and signal processing. His current research interests include signal processing, nonlinear optimization, and wireless communication. He is a member of the IEEE Communications Society. He is an Editor of the *Chinese Journal of Communications*, the *Chinese Journal of Signal Processing*, and the *Journal of China Universities of Posts and Telecommunications*.

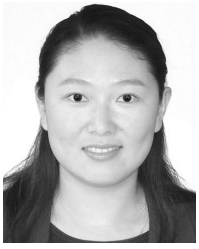

GUANNAN QU (M'10) received the B.E. degree in computer science and technology from Jinan University, Guangzhou, China, in 2003, and the M.S. and Ph.D. degrees in computer science from Jilin University, Changchun, China, in 2007 and 2010, respectively. She was financially supported by the China Scholarship Council as a Visiting Scholar with The University of Texas at Dallas, from 2008 to 2010. She is currently a Lecturer in computer science and technology with Jilin University. Her current research interests include computer system architecture, performance analysis, and quality-of-service issues in high-speed networks.

YING ZHANG (M'07–SM'15) received the M.S. degree in materials engineering from the University of Illinois at Chicago, in 2001, the M.S. degree in electrical engineering from the University of Massachusetts Lowell, in 2002, and the Ph.D. degree in systems engineering from the University of California at Berkeley, in 2006. She is currently an Associate Professor with the School of Electrical and Computer Engineering, Georgia Institute of Technology. Her current research interests include sensors and smart wireless sensing systems, power management for energy harvesting wireless sensor networks, intelligent monitoring and diagnostic systems, artificial intelligence, information retrieval and data mining, and computer-aided optimal design.

VICTOR C. M. LEUNG (S'75–M'89–SM'97–F'03) was a Professor of electrical and computer engineering and the TELUS Mobility Research Chair with The University of British Columbia (UBC), Vancouver, BC, Canada, in 2018. He is currently a Distinguished Professor of computer science and software engineering with Shenzhen University, Shenzhen, China, and a Professor Emeritus with UBC. His current research interests include wireless networks and mobile systems. He has coauthored more than 1200 journals and conference papers and book chapters. Dr. Leung is serving on the editorial boards of the IEEE Transactions on Green Communications and Networking, the IEEE Transactions on Cloud Computing, IEEE Access, the IEEE Network, and several other journals. He received the IEEE Vancouver Section Centennial Award, the 2011 UBC Killam Research Prize, the 2017 Canadian Award for Telecommunications Research, and 2018 IEEE TCGCC Distinguished Technical Achievement Recognition Award. He received the 2017 IEEE ComSoc Fred W. Ellersick Prize, the 2017 IEEE Systems Journal Best Paper Award, the 2018 IEEE CSIM Best Journal Paper Award, and the 2019 IEEE TCGCC Best Journal Paper Award for his coauthored articles. He is a Fellow of the Royal Society of Canada, the Canadian Academy of Engineering, and the Engineering Institute of Canada. He is named as Highly Cited Researchers in the current Clarivate Analytics list.